

# Optimizing Hybrid Spreading in Metapopulations

Changwang Zhang<sup>1,2,\*</sup>, Shi Zhou<sup>1,\*</sup>, Joel C. Miller<sup>4,5,6</sup>, Ingemar J. Cox<sup>1</sup>, and Benjamin M. Chain<sup>3</sup>

<sup>1</sup>Department of Computer Science, <sup>2</sup>Security Science Doctoral Research Training Centre, and <sup>3</sup>Division of Infection and Immunity, University College London, UK. <sup>4</sup>School of Mathematical Sciences, <sup>5</sup>School of Biological Sciences, and <sup>6</sup>Monash Academy for Cross & Interdisciplinary Mathematics, Monash University, Melbourne, Victoria, Australia. \*Author for correspondence (changwang.zhang.10@ucl.ac.uk or s.zhou@ucl.ac.uk)

Epidemic spreading phenomena are ubiquitous in nature and society. Examples include the spreading of diseases, information, and computer viruses. Epidemics can spread by *local spreading*, where infected nodes can only infect a limited set of direct target nodes and *global spreading*, where an infected node can infect every other node. In reality, many epidemics spread using a hybrid mixture of both types of spreading. In this study we develop a theoretical framework for studying hybrid epidemics, and examine the optimum balance between spreading mechanisms in terms of achieving the maximum outbreak size. We show the existence of *critically* hybrid epidemics where neither spreading mechanism alone can cause a noticeable spread but a combination of the two spreading mechanisms would produce an enormous outbreak. As an example we show that the 2008 outbreak of the Internet worm Conficker is a critically hybrid epidemic. Our results further suggest that the worm would have been even more infectious if it had optimised the balance between modes of spreading. Our results provide new strategies for maximising beneficial epidemics (e.g. disseminating information) and estimating the worst outcome of hybrid epidemics which damage health or economic activity.

## Introduction

Epidemic spreading phenomena are ubiquitous in nature and society. Examples include the spreading of infectious diseases within a population, the spreading of computer viruses on the Internet, and the propagation of information in society. Understanding and modelling the dynamics of such events can have significant practical impact on health care, technology and the economy. Various spreading mechanisms have been studied [1, 2]. The two most common mechanisms are *local spreading*, where infected nodes only infect a limited subset of target nodes [3]; and *global spreading*, where nodes are fully-mixed such that an infected node can infect any other node [4, 1]. For example, local spreading of infectious organisms occurs by physical contact between infected and susceptible hosts. The pattern of epidemic spread is therefore determined by the pattern of physical interaction between susceptible and infected individuals. But infections can also spread globally, for example via infectious agents which can travel great distances, and then randomly infect any individual within a large target population.

In reality, many epidemics use *hybrid spreading*, which involves a combination of two or more spreading mechanisms. Consider, for example, information propagation via both social media (local spreading) and mass media (global spreading). Social media such as Twitter or Facebook may provide rapid penetration of a selected target group, but little or no access to the majority of individuals not connected to the specified group. In contrast, mass media such as TV or newspapers can potentially deliver the information to a much bigger audience, but, the effectiveness of information transmission at an individual level (for example, its ability to alter the target individual's behaviour) may be much smaller.

Early relevant studies investigated epidemics spreading in populations whose nodes mix at both local and global levels (“two levels of mixing”) [5]. These studies did not incorporate the structure of the local spreading network, assuming both local and global spreading are fully-mixed. Since the introduction of network based epidemic analysis [3, 1], hybrid epidemics have been studied in structured populations [6], in structured households [7, 8, 9], and by considering networked epidemic spreading with “two levels of mixing” [10, 11, 12]. A number of studies [13, 14, 15, 16, 17, 18] have also considered epidemics in metapopulations, which consist of a number of weakly connected subpopulations. The studies of epidemics in clustered networks [19, 20, 21] are also relevant. Much prior work on hybrid epidemics has focused on the impact of a network's structure on spreading.

Most previous studies were about what we call the *non-critically* hybrid epidemics where a combination of multiple mechanisms is not a necessary condition for an epidemic outbreak. In this case, using a fixed total spreading effort,

a hybrid epidemic will always be less infectious than an epidemic using only the more infectious one of the two spreading mechanisms [11, 22]. However, many real examples of hybrid epidemics suggest the existence of *critically* hybrid epidemics where a mixture of spreading mechanisms may be more infectious than using only one mechanism.

In this paper we investigate whether, and if so when, hybrid epidemics spread more widely than single-mechanism epidemics. We propose a mathematical framework for studying hybrid epidemics and focus on exploring the optimum balance between local and global spreading in order to maximize outbreak size. We demonstrate that hybrid epidemics can cause larger outbreaks in a metapopulation than a single spreading mechanism. To illustrate the point, we show simulation results based on data from the outbreak of the Internet worm Conficker in 2008. Our result suggests that the worm would have been even more infectious if it had used an optimised hybrid design.

Our results suggest that it is possible to combine two spreading mechanisms, each with a limited potential to cause an epidemic, to produce a highly effective spreading process. Furthermore, we can identify an optimal tradeoff between local and global mechanisms that enables a hybrid epidemic to cause the largest outbreak. Manipulating the balance between local and global spreading may provide a way to improve strategies for disseminating information, but also a way to estimate the largest outbreak of a hybrid epidemic which can pose serious threats to health or economic prosperity.

## The Hybrid Epidemic (HE) Model

Hybrid epidemics typically take place in a *metapopulation*, consisting of a number of subpopulations. Each subpopulation is a collection of densely or strongly connected nodes, whereas nodes from different subpopulations are weakly connected. This is illustrated in Figure 1, where our model considers two spreading mechanisms: 1) local spreading where an infected node can infect nodes in its subpopulation and 2) global spreading, where an infected node can infect all nodes in the metapopulation.

In our model each subpopulation for local spreading can be either fully-mixed or a network. For mathematical convenience, we describe each subpopulation as a network and represent a fully-mixed subpopulation as a fully connected network. At each time step, an infected node has a fixed total spreading effort which must be allocated between the two spreading mechanisms. Let the hybrid tradeoff,  $\alpha$ , represent the proportion of spreading effort spent in local spreading. The proportion of global spreading effort is  $1 - \alpha$ . A tunable  $\alpha$  enables us to investigate the interaction and the joint impact of the two spreading mechanisms on epidemic dynamics, ranging from a completely local spreading scenario (with  $\alpha = 1$ ) to a completely global spreading scenario (with  $\alpha = 0$ ).

We consider the hybrid epidemic spreading in terms of the Susceptible-Infected-Recovered (SIR) model [23, 1], where each node is in one of three states: *susceptible* ( $s$ ), *infected* ( $i$ ), and *recovered* ( $r$ ). At each time step, each infected node spreads both locally and globally; it infects 1) each directly connected nodes in the same subpopulation with rate  $b_1 = \alpha\beta_1$  and 2) each susceptible node in the metapopulation with rate  $b_2 = (1 - \alpha)\beta_2$ .  $\beta_1$  is the local infection rate when all spreading effort is local ( $\alpha = 1$ ). And  $\beta_2$  is the global infection rate when all spreading effort is global ( $\alpha = 0$ ). Each infected node recovers at a rate  $\gamma$ , and then remains permanently in the recovered state. A node can infect other nodes and then recover in the same time step.

## Hybrid Spreading In A Single-Population

Before we analyse hybrid spreading in a metapopulation, we study a relatively simple case where the epidemic process takes place in a *single population*. That is, there is only one population, where local spreading is via direct connections on a network structure and global spreading can reach any node in the population.

Here we extend the system in [24] for the analysis. The system in [24] was proposed to analyse single-mechanism based epidemics for the continuous time case. Here we extend the system to analyse 1) hybrid epidemics, and 2) for the discrete time case. We calculate the probability that a random test node  $u$  is in each state: susceptible  $s(t)$ , infected  $i(t)$ , and recovered  $r(t)$ .

We denote  $p(k)$  as the probability that a node has degree (i.e. number of neighbours)  $k$ . The generating function [25] of degree distribution  $p(k)$  is defined as  $g_0(x) = \sum_k p(k)x^k$ . Let  $p_n(k)$  represent the probability that a random neighbour of  $u$  has  $k$  neighbours. We assume the network is *uncorrelated*: the degrees of the two end nodes of each

link are not correlated (i.e. independent from each other) [1]. In an uncorrelated network  $p_n(k) = p(k)k/\langle k \rangle$  [1].

Let  $\theta(t)$  be the probability that a random neighbour  $v$  has not infected  $u$  through local spreading. Let  $\vartheta(t)$  be the probability that a random node  $w$  has not infected  $u$  through global spreading. Suppose  $u$  has  $k$  neighbours, the probability that it is susceptible is  $s_k(t) = \vartheta(t)^{n-1}\theta(t)^k$  where  $n$  is the total number of nodes in the population. Then by averaging  $s_k(t)$  over all degrees, we have,

$$s(t) = \vartheta(t)^{n-1} \sum_k p(k)\theta(t)^k = \vartheta(t)^{n-1}g_0(\theta) \quad (1)$$

The probability  $\theta$  can be broken into three parts:  $v$  is susceptible at  $t$ ,  $\phi_s$ ;  $v$  is infected at  $t$  but has not infected  $u$  through local spreading,  $\phi_i$ ;  $v$  is recovered at  $t$  and has not infected  $u$  through local spreading,  $\phi_r$ . Neighbour  $v$  can not be infected by  $u$  and itself, then  $\phi_s = \vartheta^{n-2} \sum_k p_n(k)\theta^{k-1} = \vartheta^{n-2}g'_0(\theta)/g'_0(1)$ . In a time step, neighbour  $v$  1) infects  $u$  with rate  $b_1\phi_i$  through local spreading and 2) recovers without infecting  $u$  through local spreading at rate  $\gamma(1-b_1)\phi_i$ , i.e. after every time step:  $(1-\theta)$  increases by  $b_1\phi_i$  and  $\phi_r$  increases by  $\gamma(1-b_1)\phi_i$ . The increase rate of  $\phi_r$  here,  $\gamma(1-b_1)\phi_i$ , is different from that ( $r\phi_i$ ) in the original system in [24]. Because the original system was designed for the continuous time case, and in the discrete time case in this paper, neighbour  $v$  can infect  $u$  and recovers at the same time step. Given that  $\phi_r$  and  $1-\theta$  are both approximately 0 in the beginning ( $t=0$ ), we have  $\phi_r = \gamma(1-b_1)(1-\theta)/b_1$ . Then

$$\phi_i = \theta - \phi_s - \phi_r = \theta - \vartheta^{n-2} \frac{g'_0(\theta)}{g'_0(1)} - \frac{\gamma(1-b_1)}{b_1}(1-\theta) \quad (2)$$

For global spreading, the probability  $\vartheta$  can also be broken into three parts:  $w$  is susceptible at  $t$ ,  $\varphi_s$ ;  $w$  is infected at  $t$  but has not infected  $u$  through global spreading,  $\varphi_i$ ;  $w$  is recovered at  $t$  but has not infected  $u$  through global spreading,  $\varphi_r$ . Using a similar derivation process, we have  $\varphi_s = \vartheta^{n-2} \sum_k p(k)\theta^k = \vartheta^{n-2}g_0(\theta)$  and  $\varphi_r = (1-\vartheta)\gamma(1-b_2)/b_2$ , and

$$\varphi_i = \vartheta - \varphi_s - \varphi_r = \vartheta - \vartheta^{n-2}g_0(\theta) - \frac{\gamma(1-b_2)}{b_2}(1-\vartheta) \quad (3)$$

When the epidemic stops spreading,  $\phi_i = 0$  and  $\varphi_i = 0$ . By setting  $\phi_i = 0$  in equation (2) we get

$$\vartheta^{n-2} = \frac{g'_0(1)}{g'_0(\theta)} \left( \theta + \frac{\gamma(1-b_1)}{b_1}\theta - \frac{\gamma(1-b_1)}{b_1} \right) \quad (4)$$

Substituting equation (4) and  $\varphi_i = 0$  into equation (3), we have

$$\vartheta = w(\theta) = \frac{g'_0(1)(\theta + \theta\gamma(1-b_1)/b_1 - \gamma(1-b_1)/b_1)g_0(\theta)/g'_0(\theta)}{1 + \gamma(1-b_2)/b_2} + \frac{\gamma(1-b_2)/b_2}{1 + \gamma(1-b_2)/b_2} \quad (5)$$

By setting  $\phi_i = 0$  and substituting equation (5) in equation (2) we have

$$\theta = \frac{\vartheta^{n-2}g'_0(\theta)/g'_0(1) + \gamma(1-b_1)/b_1}{1 + \gamma(1-b_1)/b_1} = f(\theta) \quad (6)$$

Then  $\theta_\infty$  - stationary value of  $\theta$  is a fixed point of  $f(\theta)$ .

### Threshold Condition

$f(\theta)$  has a known fixed point of  $\theta = 1$  which represents no epidemic outbreak. We test the stability of this fixed point. By substituting equation (2) and equation (5) into  $d\theta/dt = -b_1\phi_i$ , setting  $\theta = 1 + \epsilon$  and take the leading order (Taylor Series), we have  $d\epsilon/dt = \epsilon h$  and

$$h = \frac{b_1A + b_2B + b_1b_2C - \gamma^2}{b_2 + \gamma - b_2\gamma} \quad (7)$$

where  $A = \gamma^2 + g''_0(1)\gamma/g'_0(1) - \gamma$ ,  $B = \gamma^2 + n\gamma - 3\gamma$ , and  $C = -\gamma^2 - g''_0(1)\gamma/g'_0(1) - n\gamma + 4\gamma - ng''_0(1)/g'_0(1) + 3g''_0(1)/g'_0(1) + ng'_0(1) - 2g'_0(1) + n - 3$ . Then  $\epsilon = Ce^{ht}$  where  $C$  is a constant. When  $h$  is negative,  $|\epsilon|$  gradually

decreases and approaches 0 as  $t$  increases; while when  $h$  is positive,  $|\epsilon|$  gradually increases and approaches  $+\infty$  with the increase of  $t$ . That is the fixed point  $\theta = 1$  turns from stable to unstable when  $h$  changes from negative to positive. The threshold condition for an epidemic outbreak is then  $h > 0$ :

$$h(\beta_1, \beta_2, \gamma, \alpha, p(k)) > 0, \quad (8)$$

This epidemic threshold represents an condition which, when *not* satisfied, results in an epidemic that vanishes exponentially fast [4, 26]. There are two special cases.

- For completely local spreading ( $\alpha = 1, b_1 = \beta_1, b_2 = 0$ ), the threshold reduces to  $\beta_1 g_0''(1)/[g_0'(1)(\beta_1 + \gamma - \gamma\beta_1)] > 1$ . Here  $g_0'(1) = \langle k \rangle$  and  $g_0''(1) = \langle k^2 \rangle - \langle k \rangle^2$  where  $\langle k \rangle$  is the average degree of the network and  $\langle k^2 \rangle$  is the average degree square of the network [1]. In the methods section, we show that this threshold agrees with previous threshold results [27] for single-mechanism epidemics spreading on networks for the discrete time case. For infinite scale-free networks, we have  $(\langle k^2 \rangle - \langle k \rangle^2)/\langle k \rangle \rightarrow \infty$  such that the threshold ‘vanishes’ (i.e.  $\infty > 1$  is always satisfied), in agreement with previous observation [3, 1].
- For completely global spreading ( $\alpha = 0, b_1 = 0, b_2 = \beta_2$ ), the threshold reduces to  $\beta_2(n - 3 + \gamma)/\gamma > 1$ , and when  $n$  is large it is approximate to  $\beta_2 n/\gamma > 1$ .  $\beta_2 n/\gamma$  is the basic reproduction number,  $R_0$ , for single-mechanism epidemics spreading in a fully mixed population [4].  $R_0$  is the average number of nodes that an infected node can infect before it recovers. Thus the threshold is equivalent to  $R_0 > 1$ , in agreement with previous work [4].

### Final Outbreak Size

The final outbreak size,  $r_\infty$ , is the fraction of nodes that are recovered when all epidemic activities cease, i.e. when all nodes are either recovered or susceptible. When  $t \rightarrow \infty$ , the probability that a node is infected  $i(t) \rightarrow 0$ . Thus  $r_\infty = 1 - s_\infty = 1 - \vartheta_\infty^{n-1} g_0(\theta_\infty)$  and

$$r_\infty = 1 - w(\theta_\infty)^{n-1} g_0(\theta_\infty) \quad (9)$$

where the value of  $\theta_\infty$  can be numerically calculated by conducting the fixed-point iteration of equation (6). Equation 9 can be viewed as a function of the hybrid epidemic parameters and the network degree distribution. To be noted here, for completely global spreading ( $\alpha = 0, b_1 = 0, b_2 = \beta_2$ ),  $\theta_\infty$  can not be calculated from equation (6) (because  $b_1 = 0$ ). In this case,  $\theta_\infty = 1$ ,  $g_0(\theta_\infty) = 1$ , and  $r_\infty = 1 - \vartheta_\infty^{n-1}$  where  $\vartheta_\infty$  can be obtained by setting  $\varphi_i = 0$ ,  $g_0(\theta) = 1$  and solving the equation (3) in the range  $0 < \vartheta < 1$ .

### Evaluation

Numerical simulations were performed to verify the above theoretical predictions for hybrid epidemics in a single population. We consider two typical topologies for local spreading in the single-population: (1) A fully connected network which represents a fully mixed population; (2) A random network with Poisson degree distribution, which are generated by the Erdős-Rényi (ER) model [28] with average degree 5. Each of these two networks has 1000 nodes. At the beginning, 5 randomly selected nodes are infected and all others are susceptible.

We run simulations for different values of  $\alpha \in [0, 1]$ . We set the global infection rate  $\beta_2 = 10^{-4}$  and the recovery rate  $\gamma = 1$  (i.e. an infected node only spread the epidemic in one time step). For epidemics on the fully connected network, the local infection rate  $\beta_1 = 6 \times 10^{-3}$ . And for epidemics on the random network,  $\beta_1 = 0.8$ . Figure 2 shows that the predicted final outbreak size using equation (9) is in close agreement with simulation results. It is also evident that the hybrid epidemic is characterised by a phase change, where the threshold is well predicted by equation (8). We have also conducted further evaluations for epidemics on larger networks or Power-law (PL) topology, and the results all show that our theoretical predictions have good agreement with simulations.

### Hybrid Spreading In A Metapopulation

We now extend the above theoretical results for a single-population to analyse hybrid spreading in a metapopulation which consists of a number of subpopulations. Local infection happens only between nodes in the same subpopulation whereas global infection occurs both within and between subpopulations. We use a typical metapopulation

for epidemic simulations and numerical model calculations in this section. The typical metapopulation contains 500 subpopulations and each subpopulation is a random network (generated by the ER model [28]) with 100 nodes and an average degree of 5.

### Hybrid Spreading At The Population Level

We define a subpopulation as susceptible if it contains only susceptible nodes. A subpopulation is infected if it has at least one infected node. A subpopulation is recovered if it has at least one recovered node and all other nodes are susceptible. Only global spreading enables infection between subpopulations, whereas spreading within a subpopulation can occur via both local and global spreading. The final outbreak size at the population level  $R_\infty$ , is defined as the proportion of subpopulations that are recovered when the epidemic stops spreading. We define the *population reproduction number* [14],  $R_p$ , as the average number of subpopulations that are directly infected by an infected subpopulation before it recovers. A metapopulation includes many subpopulations. In order for an epidemic to spread in a metapopulation, an infected subpopulation should infect at least one other subpopulation before it recovers, i.e. the threshold condition of the hybrid epidemic at the population-level is  $R_p > 1$ .

Figure 3 shows simulation results of the final outbreak sizes  $r_\infty$  and  $R_\infty$  and the population reproduction number  $R_p$  (right y axis) as a function of the hybrid tradeoff  $\alpha$ . Epidemic parameter values are included in Figure 3's legend. All three results show a bell shape curve regarding  $\alpha$ . It is clear that the epidemic will not cause any significant infection if it uses only local spreading ( $\alpha = 1$ ) or only global spreading ( $\alpha = 0$ ). The maximal outbreak at the node level  $r_\infty^* = 0.34$  is obtained around the optimal hybrid tradeoff  $\alpha^* = 0.5$ . That is, if 50% of the infection events occur via local spreading (and the rest via global spreading), the epidemic will ultimately infect 34% of all nodes in the metapopulation. At the population level, the total percentage of recovered subpopulations  $R_\infty$  follows a very similar trend to  $r_\infty$ , and the maximum epidemic size in terms of subpopulations occurs at the same optimal  $\alpha^*$ . The population reproduction number  $R_p$  follows a similar trend to the final outbreak sizes  $R_\infty$  and  $r_\infty$ . The threshold  $R_p > 1$  defines the range of  $\alpha$  for which the final outbreak sizes are significantly larger than zero.

It is important to appreciate that although the maximal  $R_p^*$  is uniquely defined by the optimal  $\alpha^*$ , other  $R_p$  can be obtained by *two* different  $\alpha$  values, on either side of the optimal  $\alpha^*$ , potentially representing different epidemic dynamics.

### Prediction of the Population Reproduction Number $R_p$

The population reproduction number  $R_p$  is a fundamental characteristic of hybrid epidemics in a metapopulation. We consider a metapopulation with  $N + 1$  subpopulations, which are denoted as  $p_i$  where  $i = 0, 1, 2, \dots, N$ . Each subpopulation has  $n$  nodes connected to a same structured local spreading network.  $p_0$  is the subpopulation where the epidemic starts from.

We assume the infection inside the initially infected subpopulation  $p_0$  is all caused by infected nodes inside  $p_0$ . That is, we neglect the effects of global spreading of other  $N$  subpopulations on  $p_0$ . This is an acceptable assumption when the metapopulation has a larger number of subpopulations. Under these conditions, hybrid spreading within  $p_0$  is the same as spreading in a single-population, which has been analysed in previous sections. To predict  $R_p$ , we first analyse the expected number of nodes outside  $p_0$  that will be infected by  $p_0$ . We then estimate the number of other subpopulations that these infected nodes should belong to. Let  $s_N(t)$  represent the probability that a random test node in other subpopulations are susceptible at time  $t$ . Using the same parameters defined in the analysis about hybrid epidemics in a single population, we have  $s_N(t) = \vartheta(t)^n$  where  $n$  is the number of node in  $p_0$ .

When  $p_0$  recovers at time  $T$ , the *fraction* of nodes in other subpopulations that have been infected by (infected nodes in)  $p_0$  (via global spreading) is  $x_N = 1 - s_N(T) = 1 - \vartheta(T)^n = 1 - w(\theta_T)^n$  where we have used equation (5). Then the *number* of such infected nodes is

$$X_N = x_N n N = (1 - w(\theta_T)^n) n N \quad (10)$$

where  $nN$  is the total number of nodes in other  $N$  subpopulations and  $\theta_T$  can be numerically calculated as  $\theta_\infty$  by fixed-point iteration of equation (6). As the nodes are infected randomly via the global spreading, the probability that an infected node does not belong to a particular subpopulation  $i$  is  $1 - 1/N$ ; and the probability that none of these

infected nodes belongs to the subpopulation  $i$  is  $(1 - 1/N)^{X_N}$ . So the probability that at least one infected node belongs to the subpopulation  $i$  is  $1 - (1 - 1/N)^{X_N}$ . Thus the population reproduction number  $R_p$ , which is the number of other subpopulations that these infected nodes should belong to, is:

$$R_p = N(1 - (1 - 1/N)^{X_N}) \quad (11)$$

Figure 4 compares the predicted  $R_p$  against simulation results as a function of the hybrid tradeoff  $\alpha$ .  $R_p$  is characterised by a bell-shaped curve. It peaks at the optimal hybrid tradeoff  $\alpha^*$  where the population reproduction number achieves its maximal value  $R_p^*$ . This optimal point is of particular interest as it represents the optimal trade-off between the two spreading mechanisms, where the hybrid epidemic is most infectious and therefore has the most extensive outbreak.

### The Optimal Hybrid Tradeoff $\alpha^*$ and the Maximal $R_p^*$

We next investigated the maximum epidemic outbreak in the context of varying infectivity and recovery rates. For a given set of epidemic variables, we calculate the theoretical prediction of  $R_p$  as a function of  $\alpha$  using equation (11), and then we obtain the optimal  $\alpha^*$  and the maximal  $R_p^*$ . For ease of analysis, we fix the global infection rate  $\beta_2$  at a small value of  $10^{-6}$  and then focus on the local infection rate  $\beta_1$  and the recovery rate  $\gamma$ .

Figure 5a shows the optimal hybrid tradeoff  $\alpha^*$  as a function of  $\beta_1$  and  $\gamma$ . For a given  $\gamma$ , a larger  $\beta_1$  results in a smaller  $\alpha^*$ . Intuitively this can be understood as when the efficiency of local spread increases, less effort needs to be devoted to this spreading mechanism, and more can be allocated to global spreading. On the other hand, for a given  $\beta_1$ , a larger  $\gamma$  results in an increase in  $\alpha^*$ . When the recovery rate is higher, nodes remain infectious for shorter times. In this case, in order to achieve the maximum epidemic outbreak, more local infection is favoured, since this will allow an infected subpopulation to remain infected for longer, and hence increase the probability of infecting other subpopulations before it recovers. A plot of  $\alpha^*$  versus  $\beta_1/\gamma$  is shown in Figure 5c. The fitting on a log-log scale in the inset indicates the two quantities have a power-law relationship, i.e.  $\alpha^*$  is determined by  $\beta_1/\gamma$ . This means the optimal hybrid tradeoff  $\alpha^*$  can be predicted when  $\beta_1/\gamma$  is known.

Figure 5b shows the maximal  $R_p^*$  as a function of  $\beta_1$  and  $\gamma$ , where the  $R_p^*$  is obtained when the corresponding value of  $\alpha^*$  in Figure 5a is used.  $R_p^*$  is very sensitive to the recovery rate  $\gamma$ . As  $\gamma$  approaches zero, the value of  $R_p^*$  increases dramatically (note that  $R_p^*$  uses a log-scale colour-map) regardless of value of  $\beta_1$ . This is in agreement with the intuition that a low recovery rate will favour any type of epidemic spreading. For a fixed  $\gamma$ ,  $R_p^*$  increases with  $\beta_1$ . An increased infection rate of local spreading will obviously increase the reproductive number, if other parameters are kept constant, but the effect is much smaller than that of changing the recovery rate, because global spreading maintains the reproductive number when local spreading falls to low values.

Figure 5a shows a clear phase shift between areas where an epidemic occurs (the coloured area) and areas where it does not (the white area towards the top-left corner). Accordingly, the corresponding  $R_p^*$  in Figure 5b in the area where no epidemic occurs is very small. The boundary between the epidemic and non-epidemic phase space is defined by the line  $\beta_1/(\beta_1 + \gamma - \gamma\beta_1) \approx 0.2$ . This is the threshold for completely local spreading in a single-population:  $\beta_1/(\beta_1 + \gamma - \gamma\beta_1) > g'_0(1)/g''_0(1)$  and  $g'_0(1)/g''_0(1) \approx 0.2$  for the network topology used. Since the global infection rate  $\beta_2$  is fixed at a small value, no major spreading will occur either within or between subpopulations below this threshold.

Figure 5d plots  $R_p$  as a function of  $\beta_1$  and  $\alpha$  on a log-log scale while fixing  $\gamma = 0.1$ . For given values of  $\beta_1$ , the corresponding optimal  $\alpha^*$  are shown as points. We can see that points always fall in the area of the maximal  $R_p^*$  for the given  $\beta_1$ . Each point represents a local optimum. The global optimum, the largest possible value of  $R_p$ , is obtained towards the bottom-right corner, where the local infection rate is high but the epidemic spends most effort on global spreading. Infection across subpopulations can only be achieved by global spreading. Since global spreading has a low infection rate, the epidemic should spend most of its time (or resource) on global spreading. There will be much less time spent on local spreading but its infection rate is high anyway.

### Case study on Conficker

The computer worm Conficker started spreading on the Internet on November 21, 2008 [29]. Code analysis from the antivirus company Symantec revealed that the worm uses three simple spreading mechanisms: (1) local probing

that infects computers in the same local network; (2) neighbourhood probing that infects computers in neighbouring networks; (3) global probing that randomly infects any computer on the Internet. We recently inferred [30] Conficker's parameters (infection rates, hybrid tradeoffs, recovery rate etc.) based on the Network Telescope Dataset collected by the Cooperative Association for Internet Data Analysis (CAIDA) [31, 32].

The infection rate of Conficker's global probing is extremely low, less than one successful infection in every ten million random probes across the Internet. The infection rates of local and neighbourhood probing, however, are around a million times larger than that of global probing. The difference is due to the fact that once a vulnerable node is infected, other nodes in the same local networks and neighbouring networks are very likely to have a similar level of vulnerability, and thus local and neighbouring probing becomes very effective. The worm spends around 90% of its time on global probing, which allows it to explore the Internet as widely as possible, although with a very low infection rate. Conficker has since infected more than 7 million computers and has persisted for many years [29].

We simulated Conficker outbreaks using the spreading parameters derived from the data as discussed above. For simplicity, we investigated only the interplay between local and global probing and ignored neighbourhood probing in this analysis. As shown in Figure 6, neither of the two mechanisms alone causes any outbreak (see the points at  $\alpha = 1$  and 0), whereas a hybrid spreading leads to infection of over 60% of nodes. Interestingly, when using the optimal tradeoff between the two mechanisms ( $\alpha = 0.22$ ), the worm spreads to more nodes in the simulation than the worm using all three probing mechanisms with the original parameters. A conclusion from our analysis is therefore that the worm could have been even more infectious than it actually was, by a relatively minor change to its code which optimised the allocation of probing time between global and local spreading.

## Discussion

Hybrid spreading, the propagation of infectious agents using two or more alternative mechanisms, is a common feature of many real world epidemics. Widespread epidemics (e.g. computer worms) typically spread efficiently by local spreading through connections within a subpopulation, but also use global spreading to probe distant targets usually with much lower infectivity. The amount of resources (e.g. time, energy or money) which an infectious agent can devote to each mode of propagation is necessarily limited. This study therefore focuses on the tradeoff between local and global spreading, and the effect of this tradeoff on the outbreak of an epidemic.

We develop a theoretical framework for investigating the relationships between  $\alpha$ , the relative weight given to each spreading mechanisms, and the other epidemic properties. These properties include epidemic infectivity, subpopulation structure, epidemic threshold, and population reproduction number. The predictions of the theoretical model agree well with stochastic simulation results, both in single populations and in metapopulations.

Our analysis shows that epidemics spreading in a metapopulation may be critically hybrid epidemics where a combination of the two spreading mechanisms is essential for an outbreak and neither completely local spreading nor completely global spreading can allow epidemics to propagate successfully.

Our study reveals that, in metapopulations, there exists an optimal tradeoff between global and local spreading, and provides a way to calculate this optimum given information on other epidemic parameters. We examine the predictions of the model in respect to the spread of the computer worm, Conficker, which is known to use hybrid spreading mechanisms. Our data driven simulations demonstrate that hybrid spreading is in fact an absolute requirement to explain the enormous outbreak of this worm on the Internet. Remarkably, our results suggest the worm could have been even more infectious if the tradeoff between local and global probing had been optimised.

The results of this study are of practical relevance as the total amount of time or capacity that is allocated to spreading is almost always limited by some resource constraint. For example, the total probing frequency of Internet worms is often capped at a low rate to prevent them from being detected by anti-virus software. Another example is a fixed budget for an advertisement campaign, where money can be spent on either social media (local spreading) or mass media (global spreading). Furthermore, other epidemic parameters, such as local or global infection rates are difficult to change because they derive from inherent properties of the infectious agent. For example it would be difficult to increase the global infection rate of an Internet worm. The tradeoff between different types of spreading therefore becomes a key parameter in terms of design strategy, which can be manipulated to maximise outbreak size. For

example, as we show in Figure 6, the designers of Conficker could have changed the coding to adjust the allocation of time between the probing mechanisms to make the worm even more infectious. In the context of marketing campaigns, the allocation of the total budget between different media can be adjusted to maximise the advertisement coverage.

The consideration of hybrid spreading mechanisms also has some interesting implications for strategies for protecting against the spread of epidemics. It is clear from both theoretical considerations, simulations and the behaviour of the Conficker worm, that epidemics can spread with extremely low global infection rates (far below individual recovery rates), provided there is efficient local infection. Such conditions are common for both cyber epidemics (since computers within local networks tend to share configurations) and in infectious disease epidemics, where contacts between family or community members are often much closer and more frequent than the the overall population. Protection strategies which target local networks collectively (for example intensive local vaccination around individual disease incidents, as was used in the final stages of smallpox eradication [33]) may therefore be a key element of future strategies to control future mixed spreading epidemics.

In conclusion, our study highlights the importance of the tradeoff between local and global spreading, and manipulation of this tradeoff may provide a way to improve strategies for disseminating information, but also a way to estimate the worst outcome (i.e. largest outbreak) of hybrid epidemics which can pose serious threats to health and economic prosperity.

## Methods

### Threshold for local spreading using Newman’s method

Here we use Newman’s method [27, 34, 35, 36] to obtain the threshold condition for the local spreading. Firstly we need to calculate the “transmissibility”  $T$  which is the average probability that an epidemic is transmitted between two connected nodes, of which one is infected and the other is susceptible. According to [27], for the discrete time case  $T$  can be calculated as

$$T = 1 - \int_0^{\infty} d\beta_1 \sum_{\tau=0}^{\infty} p(\beta_1) p(\tau) (1 - \beta_1)^{\tau} \quad (12)$$

where  $\tau$  is the time steps that an infected node remains infected,  $p(\tau)$  and  $p(\beta_1)$  respectively are the probability distribution of  $\tau$  and  $\beta_1$ . For the model in this paper,  $\beta_1$  is a constant and  $p(\tau) = (1 - \gamma)^{\tau-1} \gamma$ , in which  $(1 - \gamma)^{\tau-1}$  is the probability that an infected node has not recovered until  $\tau - 1$  steps after infection, and  $\gamma$  is the probability that the node recovers at the  $\tau$ th step after infection. Also for the model in this paper, each infected node at least remains infected for 1 time step. So that  $T$  for our model can be obtained as

$$T = 1 - \sum_{\tau=1}^{\infty} (1 - \gamma)^{\tau-1} \gamma (1 - \beta_1)^{\tau} = \frac{\beta_1}{\beta_1 + \gamma - \gamma \beta_1} \quad (13)$$

According to [27] the epidemic threshold for completely local spreading is  $T g_0''(1)/g_0'(1) > 1$  i.e.  $\beta_1 g_0''(1)/[g_0'(1)(\beta_1 + \gamma - \gamma \beta_1)] > 1$ . This is the same as the epidemic threshold for completely local spreading obtained in this paper.

## References

- 1 Newman, M. *Networks: An Introduction* (Oxford University Press, 2010).
- 2 Keeling, M. & Eames, K. Networks and epidemic models. *Journal of the Royal Society Interface* **2**, 295–307 (2005). WOS:000234342000003.
- 3 Pastor-Satorras, R. & Vespignani, A. Epidemic spreading in scale-free networks. *Physical Review Letters* **86**, 3200 (2001).
- 4 Anderson, R. M. Discussion: The kermack-mckendrick epidemic threshold theorem. *Bulletin of Mathematical Biology* **53**, 1–32 (1991).
- 5 Ball, F., Mollison, D. & Scalia-Tomba, G. Epidemics with two levels of mixing. *The Annals of Applied Probability* **7**, 46–89 (1997).

- 6 Vazquez, A. Epidemic outbreaks on structured populations. *Journal of Theoretical Biology* **245**, 125–129 (2007).
- 7 Ball, F. An sir epidemic model on a population with random network and household structure, and several types of individuals. *Advances in Applied Probability* **44**, 63–86 (2012).
- 8 House, T. & Keeling, M. J. Deterministic epidemic models with explicit household structure. *Mathematical Biosciences* **213**, 29–39 (2008).
- 9 Ma, J., Driessche, P. v. d. & Willeboordse, F. H. Effective degree household network disease model. *Journal of Mathematical Biology* **66**, 75–94 (2013).
- 10 Ball, F. & Neal, P. Network epidemic models with two levels of mixing. *Mathematical Biosciences* **212**, 69 (2008).
- 11 Kiss, I. Z., Green, D. M. & Kao, R. R. The effect of contact heterogeneity and multiple routes of transmission on final epidemic size. *Mathematical Biosciences* **203**, 124 (2006).
- 12 Estrada, E., Kalala-Mutumbo, F. & Valverde-Colmeiro, A. Epidemic spreading in networks with nonrandom long-range interactions. *Physical Review E - Statistical, Nonlinear, and Soft Matter Physics* **84** (2011).
- 13 Watts, D. J., Muhamad, R., Medina, D. C. & Dodds, P. S. Multiscale, resurgent epidemics in a hierarchical metapopulation model. *Proceedings of the National Academy of Sciences of the United States of America* **102**, 11157–11162 (2005).
- 14 Colizza, V. & Vespignani, A. Invasion threshold in heterogeneous metapopulation networks. *Physical Review Letters* **99**, 148701 (2007).
- 15 Mata, A. S., Ferreira, S. C. & Pastor-Satorras, R. Effects of local population structure in a reaction-diffusion model of a contact process on metapopulation networks. *Physical Review E* **88**, 042820 (2013).
- 16 Min, Y., Jin, X., Ge, Y. & Chang, J. The role of community mixing styles in shaping epidemic behaviors in weighted networks. *PLoS ONE* **8**, e57100 (2013).
- 17 Keeling, M. J., Danon, L., Vernon, M. C. & House, T. A. Individual identity and movement networks for disease metapopulations. *Proceedings of the National Academy of Sciences* **107**, 8866–8870 (2010).
- 18 Apolloni, A., Poletto, C., Ramasco, J. J., Jensen, P. & Colizza, V. Metapopulation epidemic models with heterogeneous mixing and travel behaviour. *Theoretical Biology and Medical Modelling* **11**, 3 (2014).
- 19 Miller, J. C. Spread of infectious disease through clustered populations. *Journal of the Royal Society Interface* **6**, 1121–1134 (2009).
- 20 Tildesley, M. J. *et al.* Impact of spatial clustering on disease transmission and optimal control. *Proceedings of the National Academy of Sciences* **107**, 1041–1046 (2010).
- 21 Volz, E., Miller, J., Galvani, A. & Meyers, L. Effects of heterogeneous and clustered contact patterns on infectious disease dynamics. *PLoS Computational Biology* **7** (2011).
- 22 Wang, Y. & Jin, Z. Global analysis of multiple routes of disease transmission on heterogeneous networks. *Physica A: Statistical Mechanics and its Applications* **392**, 3869–3880 (2013).
- 23 House, T. Modelling epidemics on networks. *Contemporary Physics* **53**, 213 (2012).
- 24 Miller, J. C., Slim, A. C. & Volz, E. M. Edge-based compartmental modelling for infectious disease spread. *Journal of the Royal Society Interface* **9**, 890–906 (2012). PMID: 21976638 PMCID: PMC3306633.
- 25 Newman, M. E. J., Strogatz, S. H. & Watts, D. J. Random graphs with arbitrary degree distributions and their applications. *Physical Review E* **64**, 026118 (2001).

- 26 Castellano, C. & Pastor-Satorras, R. Thresholds for epidemic spreading in networks. *Physical Review Letters* **105**, 218701 (2010).
- 27 Newman, M. E. J. Spread of epidemic disease on networks. *Physical Review E* **66**, 016128 (2002).
- 28 Erdős, P. & Rényi, A. On random graphs. i. *Publ. Math.* 290 (1959).
- 29 Shin, S., Gu, G., Reddy, N. & Lee, C. A large-scale empirical study of conficker. *IEEE Transactions on Information Forensics and Security* **7**, 676–690 (2012).
- 30 Zhang, C., Zhou, S. & Chain, B. M. Hybrid spreading of the internet worm conficker. *arXiv:1406.6046 [cs.CR]* (2014). URL <http://arxiv.org/abs/1406.6046>.
- 31 *The CAIDA UCSD Network Telescope “Three Days Of Conficker”* (Cooperative Association for Internet Data Analysis, 2008). URL [http://www.caida.org/data/passive/telescope-3days-conficker\\_dataset.xml](http://www.caida.org/data/passive/telescope-3days-conficker_dataset.xml).
- 32 *The CAIDA UCSD Network Telescope “Two Days in November 2008” Dataset* (Cooperative Association for Internet Data Analysis, 2008). URL [http://www.caida.org/data/passive/telescope-2days-2008\\_dataset.xml](http://www.caida.org/data/passive/telescope-2days-2008_dataset.xml).
- 33 De Quadros, C. C., Morris, L., Da Costa, E. A., Arnt, N. & Tigre, C. H. Epidemiology of variola minor in brazil based on a study of 33 outbreaks. *Bulletin of the World Health Organization* **46**, 165–171 (1972).
- 34 Kenah, E. & Robins, J. M. Second look at the spread of epidemics on networks. *Physical Review E* **76**, 036113 (2007).
- 35 Miller, J. C. Epidemic size and probability in populations with heterogeneous infectivity and susceptibility. *Physical Review E* **76**, 010101 (2007).
- 36 Hastings, M. Systematic series expansions for processes on networks. *Physical Review Letters* **96**, 148701 (2006).

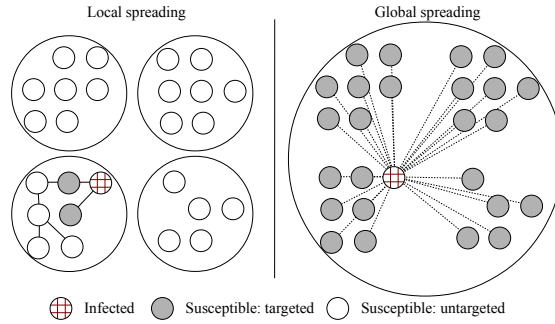


Figure 1: Hybrid epidemic spreading in a metapopulation. At each time step, an infected node has a fixed total spreading effort which must be allocated between local spreading and global spreading. The proportion of spreading effort spent in local spreading is  $\alpha$  and that in global spreading is  $1 - \alpha$ . Local spreading occurs between infected and susceptible nodes that are connected in individual subpopulations; global spreading happens between an infected node and any susceptible node in the metapopulation.

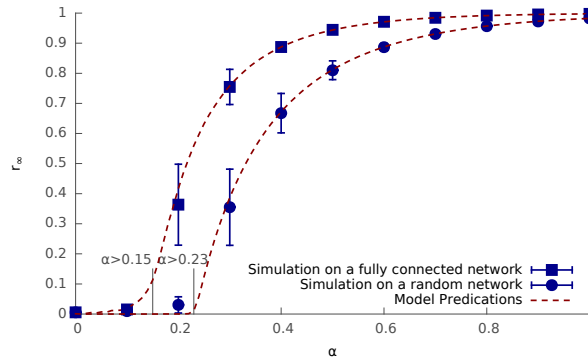


Figure 2: Final outbreak size  $r_\infty$ , as a function of the hybrid tradeoff  $\alpha$ , for hybrid epidemics in a single-population in which nodes form a fully connected network (i.e. fully mixed) or a random network with an average degree of 5. The population has 1000 nodes. The global infection rate  $\beta_2 = 10^{-4}$  and recovery rate  $\gamma = 1$  are the same for epidemics on these two types of networks. The local infection rate  $\beta_1$  is  $6 \times 10^{-3}$  for epidemics on the fully connected network; and it is 0.8 for epidemics on the random network. Initially 5 random nodes are infected. Simulation results are shown as points and theoretical predictions of equation (9) are dashed curves. The simulation results are average over 1000 runs and the bars around the points show the standard deviation. The epidemic threshold predicted by equation (8) is marked as a vertical bar.

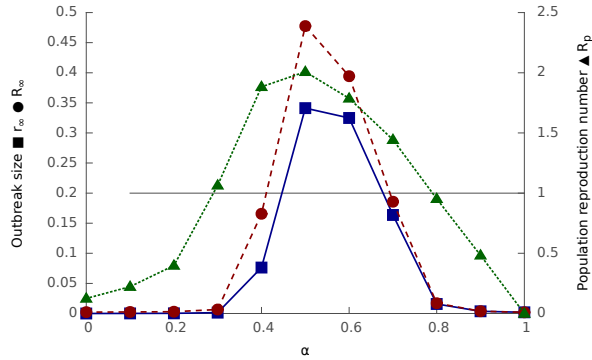


Figure 3: Simulation results of hybrid epidemics in a typical metapopulation. The three results are: (i) the final outbreak size as the fraction of recovered nodes  $r_\infty$  (squares); (ii) the final outbreak size as the fraction of recovered subpopulations  $R_\infty$  (circles); (iii) the population reproduction number,  $R_p$  (triangles, right y-axis). Each variable is plotted as a function of the hybrid tradeoff  $\alpha$ . The metapopulation contains 500 subpopulations and each subpopulation is a random network with 100 nodes and an average degree of 5. The local infection rate  $\beta_1 = 0.8$ , the global infection rate  $\beta_2 = 10^{-6}$  and the recovery rate  $\gamma = 1$ . Initially 3 random nodes in a subpopulation are infected. Simulation results are shown as points and each result is averaged over 1000 runs.

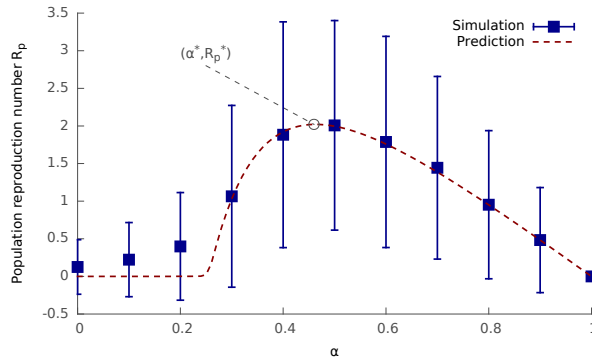


Figure 4: The population reproduction number  $R_p$  as a function of the hybrid tradeoff  $\alpha$ . Theoretical prediction from equation (11) is shown as a dashed curve. Simulation results are shown as points (average over 1,000 runs) and bars (one standard deviation). The metapopulation and epidemic parameters are the same as Figure 3.

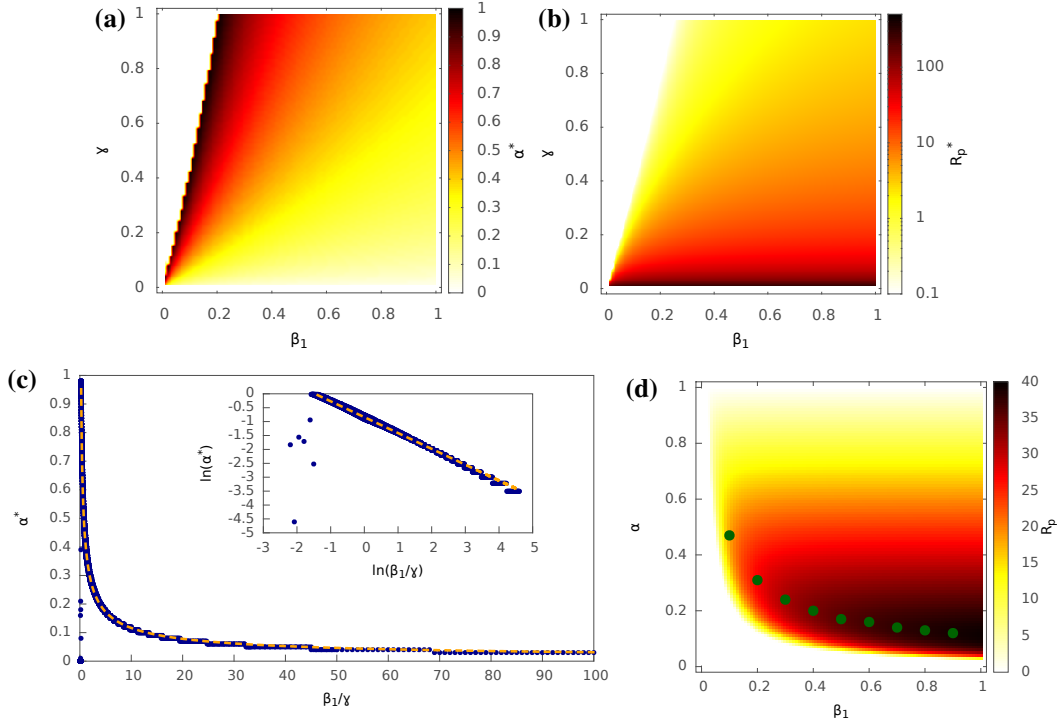


Figure 5: The estimated optimal hybrid tradeoff  $\alpha^*$  and the maximal population reproduction number  $R_p^*$  for hybrid epidemics in a typical metapopulation. (a)  $\alpha^*$  as a function of local infection rate  $\beta_1$  and recovery rate  $\gamma$ ; (b)  $R_p^*$  as a function of  $\beta_1$  and  $\gamma$ ; (c)  $\alpha^*$  as a function of  $\beta_1/\gamma$ , where the inset is on log-log scale fitted as  $\ln(\alpha^*) = -0.84 - 0.57 \cdot \ln(\beta_1/\gamma)$ . (d)  $R_p$  as a function of  $\alpha$  and  $\beta_1$  with  $\gamma = 0.1$ , where the points are the corresponding optimal  $\alpha^*$  for given  $\beta_1$ . We fix  $\beta_2 = 10^{-6}$  and the metapopulation is as in Figure 3.

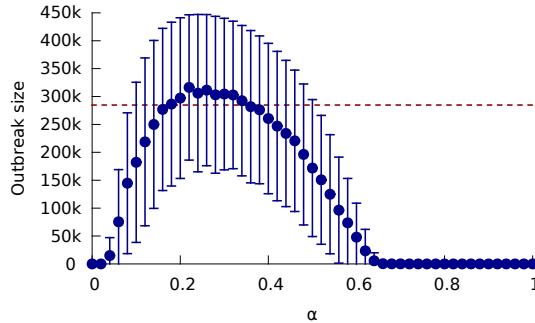


Figure 6: Simulation study on the Internet worm Conficker. The points are the average outbreak size based only on the local and global probing mechanisms as a function of the hybrid tradeoff  $\alpha$ . Simulations are run in a metapopulation containing 100,000 of 5-node subpopulations, with 2 random nodes initially infected. All results are averaged over 1000 runs. The bars represent the standard derivation. The dash line is the average outbreak size based on Conficker's three probing mechanisms with the inferred parameters (local  $\beta_l = 0.32$ ,  $\alpha_l = 5.3\%$ ; neighbourhood  $\beta_n = 0.032$ ,  $\alpha_n = 5.6\%$ ; global  $\beta_g = 7.7 \times 10^{-8}$ ,  $\alpha_g = 89.1\%$ ;  $\gamma = 6.4 \times 10^{-2}$ ).